

LASER INTERFEROMETRY

PACS numbers: 42.40.Kw; 42.70.Ln; 42.70.Nq
DOI: 10.1070/QE2011v041n09ABEH014571

Adaptive interferometry based on dynamic reflective holograms in cubic photorefractive crystals

A.A. Kolegov, S.M. Shandarov, G.V. Simonova, L.A. Kabanova, N.I. Burimov, S.S. Shmakov, V.I. Bykov, Yu.F. Kargin

Abstract. **The characteristics of a holographic interferometer, which is based on the interaction of counterpropagating light waves on reflective holograms in cubic photorefractive sillenite crystals of the (100) cut and designed for measuring surface vibration spectra from specularly reflecting objects, have been theoretically analysed and experimentally studied. The experiments showed that an interferometer of this type, based on an $Bi_{12}TiO_{20}$:Fe,Cu crystal, makes it possible to measure vibrations with an amplitude of 5 pm. An analysis performed with allowance for the shot and thermal noise of the photodetector showed that vibrations with an amplitude below 1 pm can be measured. A model is proposed to describe the experimentally found strong temperature dependence of the light interaction on reflection holograms in a $Bi_{12}TiO_{20}$:Ca crystal. This model takes into account the influence of temperature on the photoinduced charge redistribution over deep donor and shallow trap centres, as well as the drift of the interference pattern in the crystal due to the thermooptical effect and linear expansion of the crystal.**

Keywords: *cubic photorefractive crystals, reflection holograms, thermooptical effect.*

1. Introduction

Laser interferometers, which transform phase modulation of light into modulation of light intensity, make it possible to measure mechanical vibrations of reflecting surfaces with a high accuracy. The limiting sensitivity of a classical interferometer to the vibration amplitude is determined by the shot noise of the photodetector and estimated to be 10^{-15} m $Hz^{-1/2}$ for a 633-nm laser with a power of 1 mW [1]. However, such a high sensitivity may have a negative effect on real devices: an interferometric measuring system becomes affected by the environmental parameters (temperature, mechanical vibrations, pressure, etc.). In addition, the average phase shift between the signal and reference waves in interferometers must be maintained constant to provide a linear relationship between the detected signal and the vibration amplitude.

The concept of using holograms in photorefractive crystals for interferometric transformation of phase modulation into amplitude one [2] was developed in numerous studies (see, for example, [3–10]). The dynamic character of photorefractive holograms and finite operating speed of the medium during their rerecording allow one to perform adaptive processing of time-dependent light-field patterns in laser interferometers, providing both efficient phase demodulation and compensation for the low-frequency modulation caused by changes in the external conditions.

The wave interaction according to Denisiuk's scheme in cubic photorefractive crystals of sillenite family, during which efficient reflection holograms are formed due to the diffusion in the absence of applied external electric fields [10–12], is promising for these applications [6, 7, 9, 10]. The impurity optical absorption observed in sillenite crystals and its photoinduced changes depend on temperature [13]. These effects are related to thermally initiated processes of charge carrier redistribution over photoactive centres, which may lead to a change in the efficiency of reflection holograms with a change in temperature and affect the characteristics of dynamic holography devices.

In this paper we report the results of studying, both theoretically and experimentally, the amplitude characteristic of adaptive interferometer, which is based on dynamic reflection holograms formed in cubic photorefractive sillenite crystals (which possess gyrotropic properties) and is designed for measuring the vibration spectra of specularly reflecting objects. The experiments and analysis, aimed at revealing the effect of temperature on the dynamics of formation of reflection holograms and interaction of light beams on them, were performed for (100)-cut $Bi_{12}TiO_{20}$:Ca crystal.

2. Principle of holographic interferometry upon interaction of counterpropagating waves in a cubic photorefractive crystal of the (100) cut

Interaction of initial laser beams I_{s0} and I_{p0} (Fig. 1) in a photorefractive crystal leads to the formation of a dynamic hologram in it, with their simultaneous self-diffraction on it [2–12]. Here, we deal with the interference of each transmitted beam with one of the diffracted beams, i.e., the reference beam I_p interferes with I_{s1}, and I_s interferes with I_{p1}. The intensity of the signal beam transmitted through the crystal can be written as

$$I = I_0(1 + m\cos\Delta\varphi), \tag{1}$$

where $m = 2\sqrt{I_s I_{p1}}/I_0$ is the interference contrast, I_0 is the total intensity of the beams I_s and I_{p1}, and $\Delta\varphi$ is the phase shift between them. If the input signal beam I_{s0} is obtained as a

A.A. Kolegov, S.M. Shandarov, G.V. Simonova, L.A. Kabanova, N.I. Burimov, S.S. Shmakov, V.I. Bykov Tomsk State University of Control Systems and Radioelectronics, prosp. Lenina 40, 634050 Tomsk, Russia; e-mail: bykovvi@sibmail.ru;
Yu.F. Kargin A.A. Baikov Institute of Metallurgy and Materials Science, Russian Academy of Sciences, Leninsky prosp. 49, 119991 Moscow, Russia; e-mail: yu.kargin@rambler.ru

Received 25 February 2011; revision received 20 July 2011
Kvantovaya Elektronika **41** (9) 847–852 (2011)
Translated by Yu.P. Sin'kov

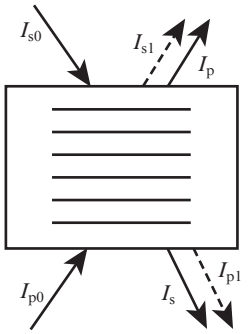

Figure 1. Holographic interferometer based on counterpropagating interaction of light beams on a photorefractive reflection hologram.

result of the reflection from an object vibrating with a frequency Ω, it is phase-modulated:

$$\Delta\varphi = \varphi_0 + \varphi_m \cos \Omega t, \tag{2}$$

and its output intensity after the interaction with the stationary reference beam on the hologram will be amplitude-modulated at multiple frequencies $n\Omega$ with a distribution of the modulation depth $M^{(n)}(\varphi_0)$ dependent on φ_0. At $\varphi_0 = 0$ or π the first harmonic is absent in the spectrum ($M^{(1)} = 0$), and quadratic phase demodulation is observed, with a maximum at the frequency 2Ω [3]. Linear phase demodulation, which is implemented at $\varphi_0 = \pi/2$ at the fundamental frequency Ω, is preferred for applications [3–9]. In this case, $m \sim \varphi_m$ at small phase modulation amplitudes.

The phase shift φ_0 for the diffracted field, which is the sum of the phase difference between the photorefractive grating and interference pattern and the additional shift for the diffraction from the phase grating, is determined by the mechanism of hologram recording. For the diffusion mechanism (in the absence of external electric field) and diffraction without a change in the polarisation state, the total phase shift is zero or π, which corresponds to quadratic phase demodulation. In the case of drift recording, when a dc electric field is applied to a crystal, and the same diffraction mode, linear phase demodulation is implemented on the phase hologram, due to the phase shift by $\pi/2$ or $-\pi/2$ [3]. However, a strong dc electric field applied to a crystal overheats the latter.

In the case of anisotropic diffraction of a light wave from a dynamic hologram, when the polarisation state of the diffracted field changes to orthogonal with respect to the initial, the linear transformation of the phase modulation of a signal wave into a change in its power may also occur for diffusion recording [6–9]. This transformation is implemented as a result of mixing of two waves with polarisations of different types: one wave must be linearly polarised, while the other must have either elliptical or circular polarisation. Linear demodulation is provided by the following: the internal phase difference ($\pi/2$) between the orthogonal components of the elliptically polarised wave is transferred into the interference of the transmitted signal wave and the diffracted field of the reference wave, thus providing a necessary additional phase shift between them.

The counterpropagating two-wave interaction of a circularly polarised stationary reference wave with a phase-modulated linearly polarised signal wave in sillenite crystals of the (100) cut was analysed in [14]. The following expressions were obtained for its intensity at the output of the crystal and for the intensity modulation depth at the zero, first, and second signal harmonics:

$$I_s(-d,t) = [M^{(0)}(-d) + M^{(1)}(-d)\sin \Omega t + M^{(2)}(-d)\cos 2\Omega t + ...](1 - R^2) I_{s0} \exp(-\alpha d), \tag{3}$$

$$M^{(0)}(-d,\varphi_m) = 1 + J_0^2(\varphi_m)\frac{\Gamma_I}{2\rho}\sin(\rho d)\left[\sin(\rho d - 2\theta_{s0}) + \frac{\Gamma_I}{4\rho}\sin(\rho d)\right], \tag{4}$$

$$M^{(1)}(-d,\varphi_m) = J_0(\varphi_m)\, J_1(\varphi_m)\frac{\Gamma_I}{\rho}\sin(\rho d)\cos(\rho d - 2\theta_{s0}), \tag{5}$$

$$M^{(2)}(-d,\varphi_m) = J_0(\varphi_m)\, J_2(\varphi_m)\frac{\Gamma_I}{\rho}\sin(\rho d)\sin(\rho d - 2\theta_{s0}), \tag{6}$$

where R is the Fresnel reflection coefficient for the crystal faces; θ_{s0} is the angle between the [010] crystallographic direction and the polarisation vector of the signal beam in the crystal at its input face; d is the crystal thickness; ρ is the specific optical rotation of the crystal; α is the light absorption coefficient; Γ_I is the gain, which characterises the beam interaction efficiency; and J_n is the nth-order Bessel function.

The advantage of the interferometer scheme under consideration is that, having chosen an appropriate input polarisation angle θ_{s0}, one can implement both linear (at $\theta_{s0} = \rho d/2 - p\pi/2$, where p is the an integer) and quadratic phase demodulation.

3. Amplitude characteristic of the adaptive interferometer based on counterpropagating interaction in a $Bi_{12}TiO20$:Fe,Cu crystal of the (100) cut

Figure 2 shows a schematic diagram of the holographic interferometer under study, which is designed for measuring the vibration spectra of specularly reflecting objects. A He–Ne laser (λ = 633 nm, power 20 mW) or a single-frequency solid-state laser (532 nm, 50 mW) were used as radiation sources. A beam-splitting cube (*2*) was used to split laser radiation into

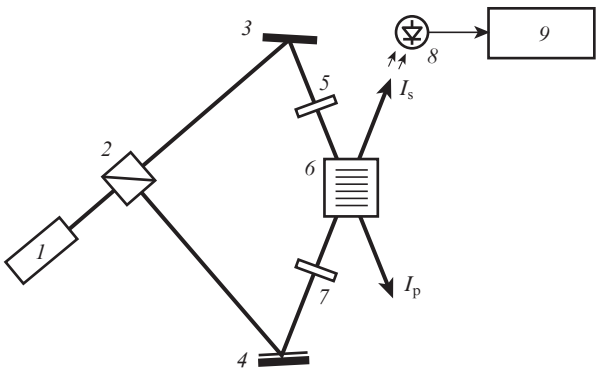

Figure 2. Schematic of a holographic interferometer based on counterpropagating interaction of waves with different polarisations: (*1*) laser, (*2*) optical splitter, (*3*) immobile mirror, (*4*) vibrating mirror, (*5*) quarter-wave plate, (*6*) photorefractive $Bi_{12}TiO_{20}$:Fe,Cu crystal of the (100) cut, (*7*) polariser, (*8*) photodiode, and (*9*) selective voltmeter.

reference and signal waves, and a quarter-wave plate (*5*) and a polariser (*7*) made it possible to set the optimal polarisation parameters of the signal and reference waves for linear phase demodulation. Phase modulation of the signal wave was performed using a mirror glued to a piezoceramic cylinder; the modulation frequency varied from 300 Hz to 10 kHz. An electric signal from a sound generator was applied to the piezoelectric ceramic through a matching transformer, and its amplitude on the cylinder was varied in limits allowing one to set the vibration amplitude of mirror (*4*) (vibrating object) from 0.005 to 300 nm. The signal wave reflected from mirror (*4*) had a much lower intensity than the reference one. After the polariser (*7*) the signal wave passed through a crystal (*6*) ($Bi_{12}TiO_{20}$:Fe,Cu, (100) cut) and arrived at a photodetector (*8*) (FD-24K photodiode, load resistance $R_L = 8.8$ kΩ, bias 12 V). The phase demodulation signal was selected at the first-harmonic frequency by a selective voltmeter (*9*) (selectivity 40 dB).

The characteristic experimental dependences of the relative amplitudes of harmonics $M^{(1)}$ and $M^{(2)}$ of the mirror vibration amplitude $l = \varphi_m\lambda/(4\pi)$ at a modulation frequency of 1.15 kHz and left circular polarisation of the pump beam ($\lambda = 532$ nm) are shown by circles in Fig. 3. The calculated dependences (curves in Fig. 3), which were found from relations (3), (5), and (6) at $\Gamma_I = 12$ cm^{-1} and $\rho = 9$ deg mm^{-1}, are in good agreement with the experimental data. As follows from these plots, in the case of counterpropagating interaction of a circularly polarised stationary reference wave with a linearly polarised signal wave in sillenite crystals of the (100) orientation, one can set both linear and quadratic regime of phase demodulation by changing the polarisation vector of the signal wave.

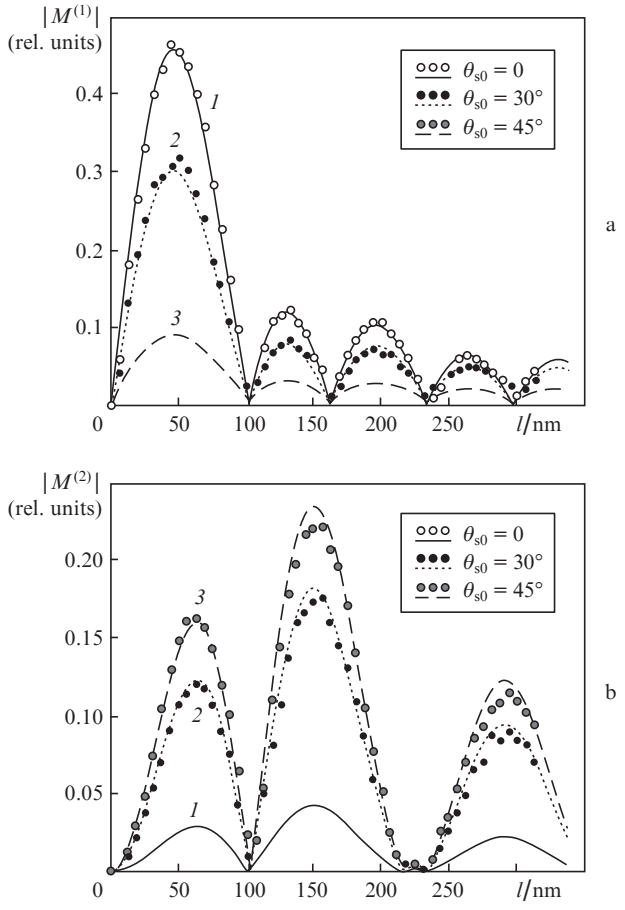

Figure 3. Dependences of the relative amplitudes of the (a) first and (b) second harmonics in the intensity modulation spectrum for a linearly polarised signal beam upon counterpropagating interaction in a $Bi_{12}TiO_{20}$:Fe,Cu crystal of the (100) cut with a circularly polarised pump wave on the reflector vibration amplitude. The input polarisation angle is θ_{s0} = (*1*) 0, (*2*) 30°, and (*3*) 45°; the vibration frequency is $f = 1.15$ kHz (circles and lines show the experimental and calculated results, respectively).

The experiments showed that the sensitivity of the interferometer based on counterpropagating wave interaction in a $Bi_{12}TiO_{20}$:Fe,Cu crystal of the (100) cut to the mirror vibration amplitude is independent of the vibration frequency in the frequency range under study (from 300 to 10^4 Hz). The typical experimental dependences of the amplitude of the electric demodulation signal (measured by the selective voltmeter on the load resistance of the photodetector) on the mirror vibration amplitude l ($f = 1.15$ kHz), obtained at the laser wavelengths $\lambda = 532$ nm (filled circles) and $\lambda = 633$ nm (empty circles), are shown in Fig. 4. One can see that the use of radiation with $\lambda = 532$ nm made it possible to measure the reflecting surface vibrations with an amplitude of 0.005 nm.

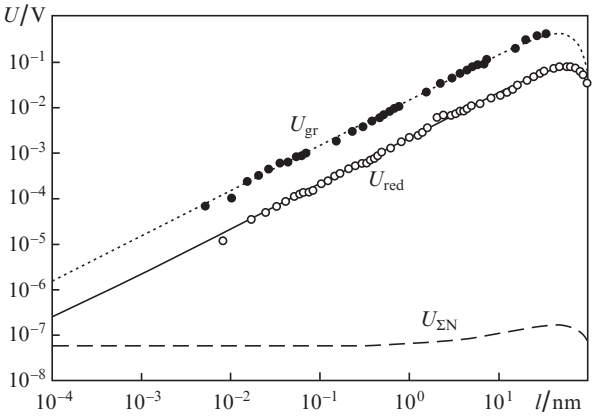

Figure 4. Dependences of the output voltage amplitude on the reflector vibration amplitude for the holographic interferometer operating with 532-nm (U_{gr}) and 633-nm (U_{red}) lasers. $U_{\Sigma N}$ is the total noise voltage; $f = 1.15$ kHz (circles and lines show the experimental and calculated results, respectively).

To determine the vibration amplitude detection limit, we will take into account the photodiode shot and thermal noise. Using the well-known relations for the photodiode detection mode [15] and formulas (3)–(5), which determine the constant component of the signal beam intensity and its first harmonic, the voltage on the selective voltmeter (to which both the signal $U_\Omega(l)$ and noise $U_{\Sigma N}$ contribute) can be written as

$$\langle U_\Omega(l) + U_{\Sigma N}\rangle = \left\{\left[R_L S_{ph} J_0(2kl) J_1(2kl)\frac{\Gamma_I}{\rho}\sin(\rho d)\right.\right.$$
$$\times \cos(\rho d - 2\theta_{s0})P_s\Big]^2 + \Delta f\Big[2eR_L^2\Big(S_{ph}\Big[1 + J_0^2(2kl)$$
$$\times \frac{\Gamma_I}{2\rho}\sin(\rho d)\Big(\sin(\rho d - 2\theta_{s0}) + \frac{\Gamma_I}{4\rho}\sin(\rho d)\Big)\Big]$$
$$\left.\left.\times P_s + I_d\Big) + 4k_B T R_L\Big]\right\}^{1/2}, \qquad (7)$$

where e is the elementary charge; S_{ph} and I_d are, respectively, the current monochromatic sensitivity and the dark current of

the photodiode; k_B is the Boltzmann constant; T is temperature; $k = 2\pi/\lambda$; $P_s = I_{s0}(1 - R^2)^2 \exp(-\alpha d)S$; S is the area of the crystal transverse cross section; and Δf is the detected frequency band.

Figure 4 shows also the calculated [from formula (7)] dependences of the measured voltage for the holographic interferometer based on lasers with $\lambda = 532$ nm (dotted line) and $\lambda = 633$ nm (solid line), as well as the dependence $\langle U_{\Sigma N}(l) \rangle$ (dashed line). The calculations were performed using the reference data for the FD-24K photodiode ($S_{ph} = 0.4$ A W^{-1}, $I_d = 1.2$ μA [16]) and the parameters of the working crystal ($R = 0.19$, $d = 1.15$ mm); the experimental values $\rho = 9$ deg mm^{-1}, $\Gamma_I = 12$ cm^{-1}, and $\alpha = 10$ cm^{-1} (for $\lambda = 532$ nm) and $\rho = 6.34$ deg mm^{-1}, $\Gamma_I = 2.04$ cm^{-1}, and $\alpha = 1$ cm^{-1} ($\lambda = 633$ nm); and the angles set in the experiments: $\theta_{s0} = 0$ ($\lambda = 532$ nm) and $\theta_{s0} = 8°$ ($\lambda = 633$ nm). For the 532-nm laser the signal input power $P_{s0} = I_{s0}S$ was estimated to be 0.2 mW, whereas for the helium–neon laser it was ~0.04 mW. As can be seen in Fig. 4, the holographic interferometer under study can be used to analyse vibrations with an amplitude of 1 pm or less.

4. Influence of temperature on the formation of reflective holograms in sillenite crystals

Due to the high sensitivity of the interferometer to the signal beam phase variations, the crystal temperature may affect significantly the device characteristics. The influence of the temperature of bismuth titanate crystal on the formation of reflection holograms in it was analysed on an experimental setup similar to that used in [17]; it was supplemented with a Peltier heater and a temperature control unit [13].

The interferometer sensitivity to temperature variations increases with an increase in the crystal thickness. Therefore, we will describe the experiments where a reflection hologram was formed in a $Bi_{12}TiO_{20}$:Ca crystal [(100) cut, thickness $d = 5.9$ mm] by the interference pattern of the pump light beam (He–Ne laser, $\lambda = 633$ nm) passing through the crystal and the signal beam reflected from the crystal output face (with the coordinate $x = 0$). In this case, the phase difference of the interfering beams for $x = 0$ remains constant when external conditions (including crystal temperature) change. Measurement of the time dependences of the intensities of the pump beam, $I_p(t)$, and the signal beam transmitted through the input face ($x = -d$) in the direction close to counterpropagating, $I_s(t)$, allowed us to calculate the evolution of the gain $\Gamma_I(t)$ for the reflection hologram from the known relations [6, 12].

In the experiments aimed at forming a reflection photorefractive hologram at a fixed temperature the crystal was heated in darkness to a specified temperature and then maintained at this temperature with an error of ±1 °C. Furthermore we switched on the pump beam and recorded the changes in the intensities $I_p(t)$ and $I_s(t)$ with time, which were caused by the hologram formation and photoinduced changes in the light absorption in the crystal.

The time dependences of the gain, $\Gamma_I(t)$, at crystal temperatures of 25 and 40 °C, calculated from the experimental data, are shown in Fig. 5. The fluctuations of the reflection hologram efficiency, whose relative amplitude increases with an increase in the crystal temperature, are due to the operation of the control unit, which alternately switches the Peltier module off and on to maintain the specified temperature. With an increase in the crystal temperature to 40 °C the dependence of the average gain becomes nonmonotonic, and its maximum value decreases. This behaviour indicates a strong influence

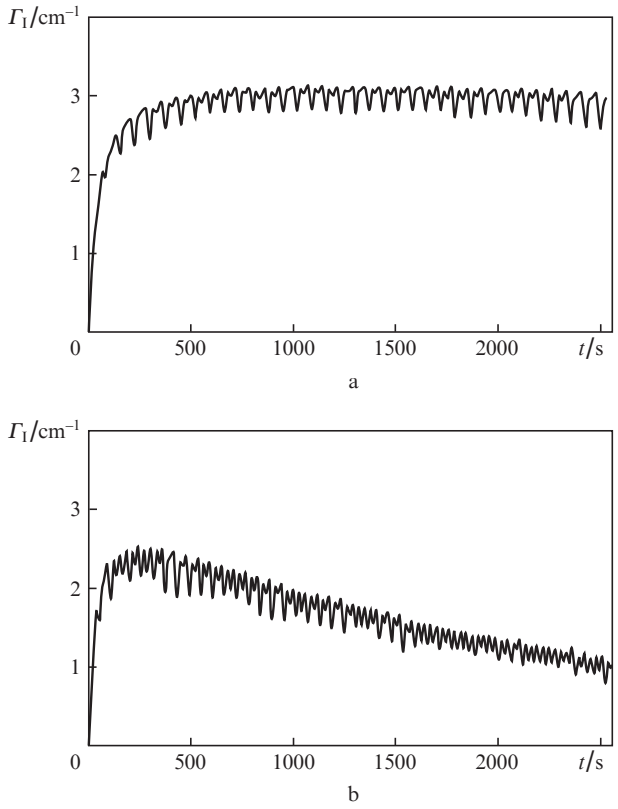

Figure 5. Time dependences of the gain during the formation of a reflection photorefractive hologram in a $Bi_{12}TiO_{20}$:Ca crystal of the (100) cut for crystal temperatures of (a) 25 and (b) 40 °C.

of temperature on the counterpropagating interaction of light beams on reflection holograms in bismuth titanate.

To exclude the influence of the Peltier module switching on the temperature characteristics of the interaction under study, we performed experiments in which the crystal was first heated in darkness to a specified temperature, then heating was stopped, and the pump beam was switched on to form a dynamic hologram. The time dependence of the gain, $\Gamma_I(t)$, of the reflection hologram upon cooling the crystal preliminarily heated to 40 °C, which was calculated based on the experimental data, is shown in Fig. 6. An analysis of the behaviour of the two-beam interaction efficiency on a reflection grating with a change in temperature (Figs 5, 6) shows that one must

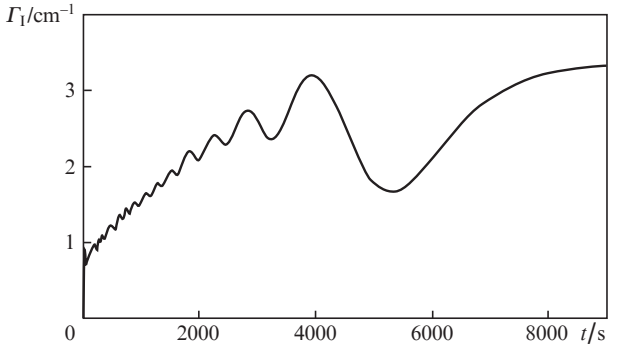

Figure 6. Time dependence of the gain during the formation of a reflection photorefractive hologram in a $Bi_{12}TiO_{20}$:Ca crystal of the (100) cut upon cooling the crystal from 40 °C.

take into account the influence of the crystal temperature on both the processes of charge redistribution over defects and the drift of the interference pattern in the crystal due to the thermooptical effect and linear expansion.

The influence of temperature on the charge redistribution over defects will be analysed within the band transport model. This model assumes that both deep donor–trap pairs [13] (which provide only photoexcitation of electrons to the conduction band) and shallow traps (occupied as a result of the recombination of these electrons from the conduction band) are present in sillenite crystals. The occupation of traps and, correspondingly, the increase in the effective number of trap centres [18], lead to expansion of the effective space-charge field of the hologram. The establishment of equilibrium for the thermal and optical excitation of electrons from shallow traps to the conduction band may be responsible for the increase in the effective number of trap centres with a decrease in temperature.

The redistribution of electrons over donor and trap centres was described using the kinetic equations [13, 18]. When analysing the first harmonic of the space-charge field, which contributes to the counterpropagating interaction under consideration, the first factor that must be taken into account is that the change in the crystal temperature T due to the thermooptical effect changes its refractive index n_0 [19]:

$$n_0(t) = n_0 + \frac{\mathrm{d}n_0}{\mathrm{d}T}\Delta T(t), \tag{8}$$

(note that the coefficient $\mathrm{d}n_0/\mathrm{d}T > 0$ for sillenite-family crystals). As a result, the spatial period of the interference pattern depends on time:

$$\Lambda(t) = \frac{2\pi}{|\boldsymbol{K}(t)|} = \frac{2\pi}{2kn_0(t)} = \frac{\lambda}{2n_0(t)}, \tag{9}$$

where $\boldsymbol{K}$ is the photorefractive-grating vector (directed along the x axis).

Second, the thermal extension of the crystal along the x axis shifts the charge gratings formed in it with respect to this dynamic interference pattern. In the case under consideration (the intensity distribution for the light field formed as a result of the interference of the pump beam with the signal beam reflected from the face $x = 0$), this face can be considered as 'fixed' with respect to the origin of coordinates. Here, the current coordinate x' along the x direction, which determines the instantaneous charge on the defects at some local crystal point, is a function of time:

$$x' = [1 + \alpha_t \Delta T(t)]x, \tag{10}$$

where α_t is the linear expansion coefficient.

In the approximation of small contrasts of the interference pattern that forms a hologram, the system of equations corresponding to the model analysed here is linearised by expanding the unknown functions F in the Fourier series, taking into account the thermooptical effect and shift of charge gratings due to linear expansion of the crystal:

$$F(x', t) = F_0(t) + \frac{F_1(t)}{2}\exp\{\mathrm{i}2k_0n_0(t)x'/[1 + \alpha_t\Delta T(t)]\} + \frac{F_1^*(t)}{2}\exp\{-\mathrm{i}2k_0n_0(t)x'/[1 + \alpha_t\Delta T(t)]\}. \tag{11}$$

Using the well-known technique (see, for example, [3, 20]), we obtained a closed system of equations for zero spatial harmonics and solved it numerically. To analyse the dynamics of the first spatial harmonics of the charge gratings and the space-charge field $E^{(1)}(t)$, we developed a technique modelling the change in temperature. The characteristic time dependence for $E^{(1)}(t)$, which assumes that the crystal temperature was maintained at the level $T = 341 \pm 1$ K up to the instant $t = 3000$ s and decreased according to the exponential law at $t > 3000$ s, is shown in Fig. 7. At $t = 2000$ s the pump beam was switched on simultaneously with the signal beam, which allowed us to model the formation of a reflection grating and calculate the dependence $E^{(1)}(t)$ at a specified mode of crystal temperature evolution.

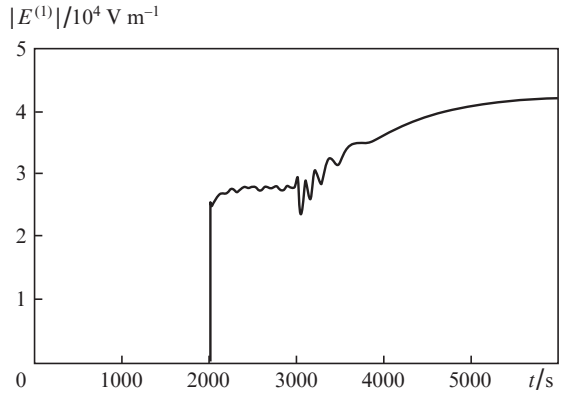

Figure 7. Time dependence of the modulus of the first-harmonic amplitude for the space-charge field $|E^{(1)}(t)|$ of a reflection hologram in a bismuth titanate crystal upon changing temperature. In the time interval $0 < t < 2000$ s the crystal is heated to the temperature $T = 341 \pm 1$ K in the absence of a light beam, at $t = 2000$ s a light beam is switched on to form a reflection hologram, in the interval $2000 < t < 3000$ s the temperature is maintained at the level $T = 341 \pm 1$ K, and at $t > 3000$ s the crystal temperature decreases exponentially.

As follows from the comparison of Figs 5–7, the theoretical model proposed here describes qualitatively the experimentally observed behaviour of the gain $\Gamma_1(t) \propto E^{(1)}(t)$ with a change in the temperature of the bismuth titanate crystal.

5. Conclusions

It was demonstrated experimentally that the holographic interferometer based on counterpropagating interaction of light waves on reflection holograms in a cubic photorefractive $Bi_{12}TiO_{20}$:Fe,Cu crystal of the (100) cut can be used to measure vibrations with an amplitude of 5 pm at frequencies from 300 Hz to 10 kHz. An analysis of the amplitude characteristics of this interferometer, which was performed taking into account the shot and thermal noise of the photodetector, showed that vibrations with amplitudes less than 1 pm can be measured.

A strong temperature dependence of the efficiency of counterpropagating light wave interaction on reflection holograms in a $Bi_{12}TiO_{20}$:Ca crystal of the (100) cut is experimentally found. A theoretical model is proposed, which takes into account the influence of temperature on the photoinduced charge redistribution over deep donor–trap and shallow trap centres, as well as the drift of the interference pattern in the crystal due to the thermooptical effect and linear expansion.

Acknowledgements. This study was supported by the Program 'Development of the Higher School Scientific Potential' for 2009–2010 and the Federal Targeted Program 'Scientific and Scientific-Pedagogical Personnel of Innovative Russia' (State Contract No. 02.740.11.0553).

References

1. Wagner J.W., Spicer J.B. *J .Opt. Soc. Am. B*, **4**, 1316 (1987).
2. Hall T.J., Fiddy M.A., Ner M.S. *Opt. Lett.*, **5**, 485 (1980).
3. Petrov M.P., Stepanov S.I., Khomenko A.V. *Fotorefraktivnye kristally v kogerentnoi optike* (Photorefractive Crystals in Coherent Optics) (St. Petersburg: Nauka, 1992).
4. Stepanov S.I. *Rep. Prog. Phys.*, **57**, 39 (1994).
5. Solymar L., Webb D.J., Grunnet-Jepsen A. *The Physics and Application of Photorefractive Materials* (Oxford: Clarendon Press, 1996).
6. Shandarov S.M., Burimov N.I., Kul'chin Yu.N., Romashko R.V., Tolstik A.L., Shepelevich V.V. *Kvantovaya Elektron.*, **38**, 1059 (2008) [*Quantum Electron.*, **38**, 1059 (2008)].
7. Kamshilin A.A., Romashko R.V., Kulchin Yu.N. *J. Appl. Phys.*, **105**, 031101 (2009).
8. Petrov V.M., Petrov M.P., Bryksin V.V., Peter E, Chudi T. *Zh. Eksp. Teor. Fiz.*, **131**, 798 (2007).
9. Romashko R.V., Kul'chin Yu.N., Kamshilin A.A. *Izv. Ross. Akad. Nauk, Ser. Fiz.*, **70**, 1296 (2006).
10. Kukhtarev N., Chen Bo Su, Venkateswarlu P., Salamo G., Klein M. *Opt. Commun.*, **104**, 23 (1993).
11. Mallick S., Miteva M., Nikolova L. *J. Opt. Soc. Am. B*, **14**, 1179 (1997).
12. Plesovskikh A.M., Shandarov S.M., Mart'yanov A.G., Manndel' A.E., Burimov N.I., Shaganova E.A., Kargin Yu.F., Volkov V.V., Egorysheva A.V. *Kvantovaya Elektron.*, **35**, 163 (2005) [*Quantum Electron.*, **35**, 163 (2005)].
13. Shandarov S.M., Polyakova L.E., Mandel A.E., Kisteneva M.G., Vidal J., Kargin Yu.F., Egorysheva A.V. *Proc. SPIE Int. Soc. Opt. Eng.*, **6595**, 124 (2007).
14. Shandarov S.M., Kolegov A.A., Burimov N.I., Bykov V.I., Petrov V.M., Kargin Yu.F. *Phys. Wave Phenomena*, **17**, 39 (2009).
15. Anisimova I.D., Vikulin I.M., Zaitov F.A., Kurmashev Sh.D. *Poluprovodnikovye fotopriemnikii ul'trafioletovyi and vidimyi i blizhnii infrakrasnyi diapazony spektra* (Semiconductor Photodetectors: UV, Visible, and Near-IR Spectral Ranges) (Moscow: Radio i svyaz', 1984).
16. Aksenenko M.D., Baranochnikov M.L. *Priemniki opticheskogo izlucheniya. Spravochnik* (A Hanbook of Light Detectors) (Moscow: Radio i svyaz', 1987).
17. Mart'yanov A.G., Ageev E.Yu., Shandarov S.M., Mandel' A.E., Bochanova N.V., Ivanova N.V., Kargin Yu.F., Volkov V.V., Egorysheva A.V., Shepelevich V.V. *Kvantovaya Elektron.*, **33**, 226 (2003) [*Quantum Electron.*, **33**, 226 (2003)].
18. Shandarov S.M., Kobozev O.V., Reshet'ko A.V., Krauze M.G., Volkov V.V., Kargin Yu.F. *Ferroelectrics*, **202**, 257 (1997).
19. Babonas G.A. in *Elektrony v poluprovodnikakh. Elektronnaya struktura i opticheskie spektry poluprovodnikov* (Electrons in Semiconductors. Electronic Structure and Optical Spectra of Semiconductors) (Vil'nyus: Mokslas, 1987) Iss. 6, p. 41.
20. Shandarov S.M., Shandarov V.M., Mandel' A.E., Burimov N.I. *Fotorefraktivnye effekty v elektroopticheskikh kristallakh* (Photorefractive Effects in Electro-Optical Crystals) (Tomsk: Izd-vo Tomsk. Gos. Univ. Sistem Upravleniya i Radioelektroniki, 2007).